



12th IEA Heat Pump Conference 2017



Analytical model of a multichannel double tube CO₂ gas-cooler for a water heater

Hanseok Mun^a, Keongsoo Song^b, Sunjae Kim^b, Joo Seong Lee^b, Yongchan Kim^{c,*}

^{a,b}A Graduate School of Mechanical Engineering, Korea University, Anam-Ro, Sungbuk-ku, Seoul, 136-701, Republic of Korea

^cA School of Mechanical Engineering, Korea University, Anam-Ro, Sungbuk-ku, Seoul, 136-701, Republic of Korea

Abstract

In a CO₂ water heater system, a water-CO₂ double tube gas-cooler is an important component affecting the system performance. Due to the variation in the thermal properties of supercritical CO₂ with the temperature, it is important to carefully design the gas-cooler used in the water heater. In this study, an analytical model of the water-CO₂ double tube gas-cooler having several inner channels was developed using the finite-volume method. The gas-cooler model was validated by the experimental data for three gas-coolers having 2, 4, 8 inner tubes. To estimate the gas-cooler performance according to the number of inner tubes, the cross-sectional area ratio between the inner tubes and outer tube of the gas-cooler was defined, which was called as 'GCAR'. The heat transfer rate and thermal effectiveness of the gas cooler were analyzed according to the GCAR. For the maximum heating capacity, the optimum design of the gas-cooler was suggested and the optimum operating conditions of the CO₂ water heater system were recommended.

© 2017 s HPC 2017.

Selection and/or peer-review under responsibility of the organizers of the 12th IEA Heat Pump Conference 2017.

Keywords : CO₂, Gas-cooler, Cross-sectional area of the gas-cooler, Water heater, Double-tube heat exchanger;

1. Introduction

Along with the European nations' banning of the high GWP HFC refrigerants, HFO and natural refrigerants are gaining attention for heating and cooling applications. Especially, a natural refrigerant, CO₂ has numerous advantages; economically reasonable, non-toxic, and inflammable. With the advantages, CO₂ is considered as an alternative refrigerant for future refrigeration systems. For the commercialization of the CO₂ cycle, the cycle

* Corresponding author. Tel.: +82-2-3290-3366; fax: +82-2-921-5946.

E-mail address: yongckim@korea.ac.kr .

should be studied with the consideration of the physical properties of CO₂ in the super critical region. Kauf^[1] suggested the pressure in the gas cooler according to the outdoor temperature of the gas cooler. Cecchinato et al.^[2] developed a simulation model of a water to CO₂ gas cooler and optimized the pressure condition of the gas cooler. Sanchez et al.^[3] used a finite simulation model and optimized the number of the segments of the finite model in the gas cooler to estimate the thermal effectiveness of the heat exchanger.

In this study, the finite volume model of a gas cooler with different number of inner channels was developed for a 4 kW water heater. In addition, the simulation model was validated using the experiment data. Overall, the cross-sectional area ratio of the gas cooler was optimized by estimating the heating capacity of the water heater system.

2. Experimental setup and testing method

Fig.1 shows a schematic diagram of the experimental setup for the CO₂ water heater system. The system consisted of two main parts; a CO₂ loop and a water loop. The CO₂ loop consisted of a scroll compressor, counter flow gas cooler, EEV, and electric heaters as an evaporator. The water loop consisted of a constant temperature bath and the gas-cooler. The pressure and temperature of CO₂ and water at the inlet and outlet of each component were measured by the pressure transducers and T-type thermocouples, respectively. The flow rates of CO₂ and water were measured by a mass flow meter and volumetric flow meter, respectively. The water-CO₂ gas-cooler has counter flow, and 5 thermocouples were attached along the gas-cooler. The gas-cooler pressure, compressor speed, water inlet temperature, volumetric flow rate, and the gas-cooler cross-sectional area ratio (GCAR) were considered as the independent variables of the experiments. The GCAR was defined as the area ratio between the cross sectional area of the inner tubes and the cross-sectional area of the outer tube, which is given in Eq. (1). Table.1 shows the range of the experimental parameters. In all tests, the superheat of CO₂ at the compressor suction was fixed at 10 °C.

Three gas-coolers were used in the experiments with various GCAR. The number of inner-tubes at each gas-cooler was 2, 4, 8, and the diameter of the outer-tube was fixed for all gas-coolers. To minimize the effect of the surface area on the heat transfer rate, all gas-coolers were designed to have equal heat transfer area. The geometric information and schematic diagram of the three gas-coolers were presented in Table. 2 and Fig. 2, respectively.

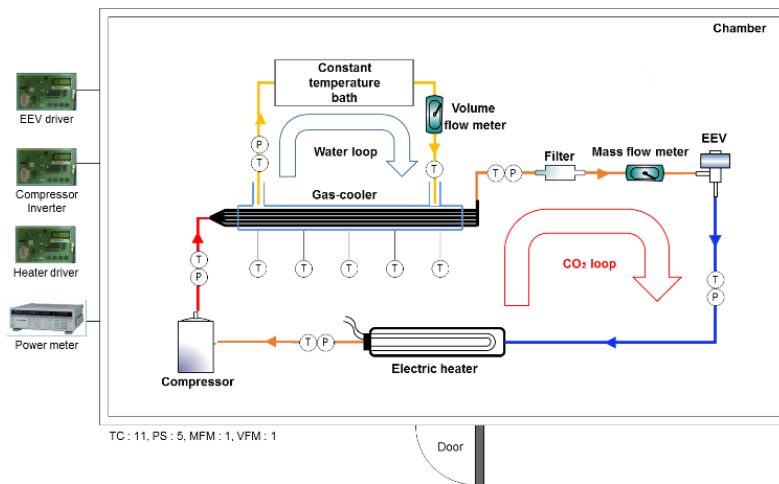


Fig. 1 Schematic diagram of the CO₂ water heater for the experiments.

Table 1. Range of the experimental data.

Variable	Min	Max	Uncertainty
P_{gc} (kPa)	7466	9601	± 40 kPa
P_{cv} (kPa)	2998	6750	± 40 kPa
$T_{CO_2, gc, i}$ ($^{\circ}C$)	50.9	92.8	± 0.5 $^{\circ}C$
$T_{CO_2, gc, o}$ ($^{\circ}C$)	18.5	48.8	± 0.5 $^{\circ}C$
$T_{w, gc, i}$ ($^{\circ}C$)	13.7	33.9	± 0.5 $^{\circ}C$
$T_{w, gc, o}$ ($^{\circ}C$)	19.9	45.9	± 0.5 $^{\circ}C$
\dot{m}_{CO_2} (kg/s)	0.0126	0.0401	± 0.5 % of reading
\dot{V}_w (l/min)	3.98	8.11	± 0.35 % of reading
Compressor speed (rpm)	2700	3600	-
$Re_{CO_2, i}$	82846	519464	-
$Re_{w, i}$	1462	5194	-
Charge amount of CO_2 (g)	600		-

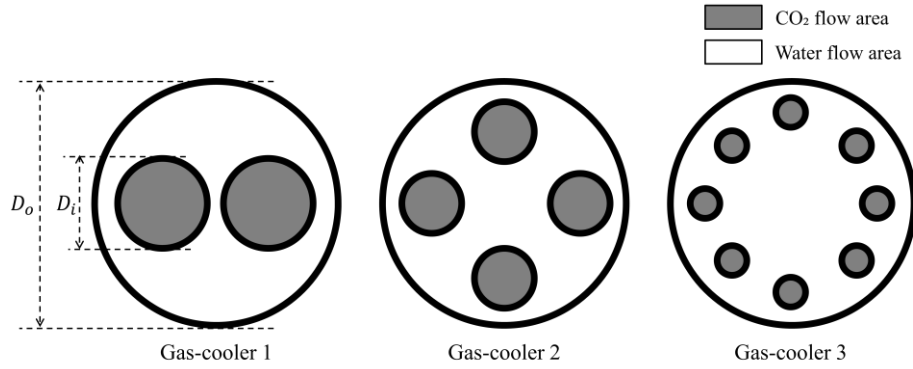


Fig. 2. Cross-sectional view of the double-tube gas-cooler used in the experiments.

Table 2. Geometrical information of the gas-coolers used in the experiments.

Geometrical variable	Gas-cooler 1	Gas-cooler 2	Gas-cooler 3
Outer tube diameter (D_o , mm)		25.4	
Outer tube thickness (Th_o , mm)		1	
Inner tube diameter (D_i , mm)	9.52	6.35	3.15
Inner tube thickness (Th_i , mm)		0.6	
Inner tube number (n)	2	4	8
Gas-cooler length (L, m)		2	
Heat exchange surface area (A_{sf} , m^2)	0.119	0.159	0.158
Cross-sectional area ratio (σ)	0.216	0.166	0.047

$$\sigma = \frac{\sum_{j=1}^n A_{cr, i, j}}{A_{cr, o}} = \frac{n \times A_{cr, i}}{A_{cr, o}} \quad (1)$$

3. Development of a finite-volume gas-cooler model

Fig. 3 shows the flow chart of the water heater simulation model. $T_{w,gc,i}$, P_{gc} , V_w , rpm, and gas-cooler geometry were used as the input. $T_{CO_2,gc,o}$, and P_{ev} were assumed for the first iteration. From the first two-steps of the simulation, the CO_2 temperature at the gas-cooler inlet ($T_{CO_2,gc,i}$) and the compressor isentropic efficiency (η_{isen}) were calculated. These values were evaluated by an artificial neural-network model using the Levenberg-Marquardt algorithm ('trainlm' function in MATLAB R2016a) based on 103 cases of the experimental data. The R-squared of the neural-network model of $T_{CO_2,gc,i}$ and η_{isen} were 0.987 and 0.993, respectively. P_r , P_{gc} , rpm, $T_{w,gc,i}$, V_w , σ were used as the input of the neural-network model.

$T_{CO_2,gc,i,sim}$ and the CO_2 temperature at the gas-cooler inlet were calculated from $T_{CO_2,gc,o,as}$, which was assumed to be the CO_2 temperature at the gas-cooler outlet, by the finite volume model of the gas-cooler. When the difference between $T_{CO_2,gc,i,sim}$ and $T_{CO_2,gc,i}$ was smaller than the pre-designed error, the iteration of the simulation was terminated. However, when the difference was larger than the pre-designed error, $T_{CO_2,gc,o,as}$ was adjusted using the Newton-Raphson method.

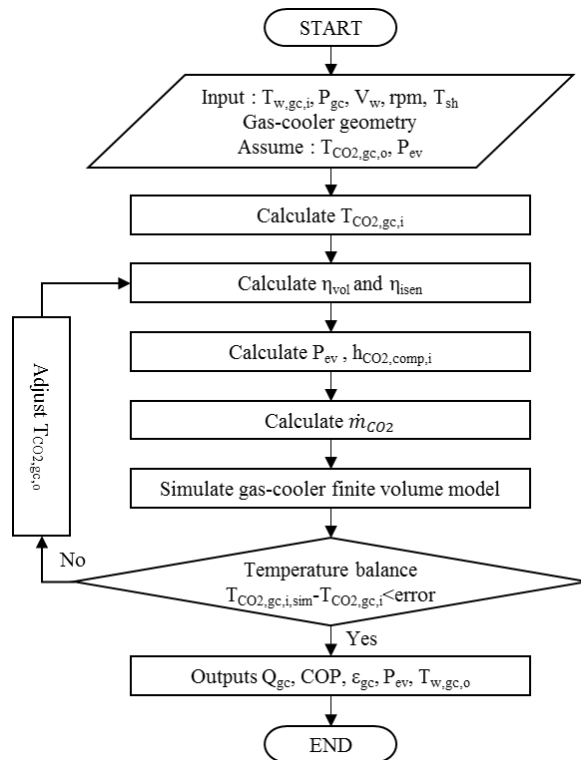


Fig. 3. Flow chart of the water heater simulation model.

Fig. 4 shows the finite element of the gas-cooler model. The total number of the finite volume segment is 50. 'i-1'th segment's output was used as the input of the 'i'th segment. To calculate the heat transfer coefficient of the gas-cooler, the Gnielinski^[4] correlation, the Stephan^[5] correlation, and the Gnielinski^[6] correlation were utilized for modeling of CO_2 turbulent flow, water laminar flow, and water turbulent flow, respectively.

To validate the simulation model, the heating capacity and water outlet temperature of the gas-cooler were compared with the experimental data (103 data points). The maximum difference for the water outlet temperature of the gas-cooler was 2.62 °C. Fig. 5 compares the heating capacity obtained from the simulated model with the experimental data. The predicted heating capacity was consistent with the measured data with the maximum deviation of 10%.

4. Simulation results and discussion

Fig. 6(a) shows the gas-cooler heating capacity according to the GCAR. When the water inlet temperatures were 25 °C and 35 °C, the heating capacity increased with a decrease in the GCAR. However, at the water inlet temperature of 15 °C, the heating capacity decreased with a decrease in the GCAR for the GCAR lower than 0.12. Fig. 6 (b) shows the thermal effectiveness of the gas-cooler according to the GCAR. The thermal effectiveness

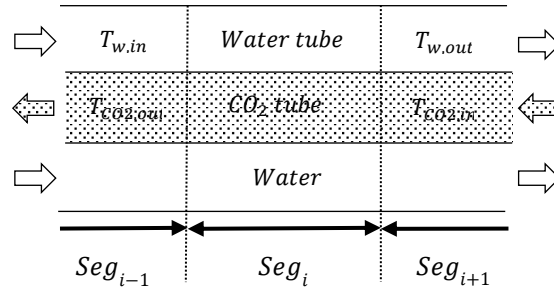


Fig. 4. Finite element of the gas-cooler model.

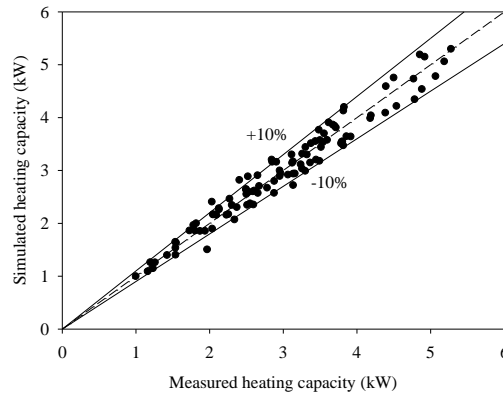


Fig. 5. Comparison of the measured heating capacity with the predictions.

of the gas-cooler was defined as Eq. (2). The thermal effectiveness decreased with an increase in the GCAR. The heating capacity and the thermal effectiveness of the gas-cooler showed similar trend according to the GCAR except for the water inlet temperature of 15 °C. At the water inlet temperature of 15 °C, the heating capacity rather decreased despite the increase in the thermal effectiveness of the gas-cooler. This can be explained with the mass flow rate and the heat transfer coefficient of the gas-cooler. Fig. 7 (a) shows the heat transfer coefficient in the gas-cooler and Fig. 7 (b) show the mass flow rate of the CO₂ cycle. The decrease in the mass flow rate of the CO₂ cycle was larger than the increase in the overall heat transfer coefficient in the gas-cooler at the water inlet temperature of 15°C. Due to the large decrease in the mass flow rate, the total heating capacity in the gas-cooler decreased in spite of the increase in the overall heat transfer coefficient.

Due to the decrease in the evaporating pressure, the mass flow rate of CO₂ decreased. With the inlet water temperature lower than the pseudo-critical temperature of CO₂, the density of CO₂ at the gas-cooler outlet increased rapidly. Due to the high density of CO₂, a large amount of the refrigerant was stagnated in the high pressure side between the gas-cooler outlet and the EEV inlet. Consequently, the refrigerant in the low pressure side decreased, causing the decrease in the evaporating pressure and reduction in the density of CO₂ at the compressor inlet. Therefore, the mass flow rate of the CO₂ cycle decreased. Fig. 8 shows the amount of the refrigerant in the high pressure side of the system according to the GCAR. The heating capacity decreased until the refrigerant amount in the high pressure side was larger than 360 g.

To prevent the decrease in the heating capacity and maximize the thermal effectiveness of the gas-cooler, it is required to design the gas-cooler having the low GCAR of 0.05 and the CO₂ temperature at the gas-cooler outlet above the pseudo-critical temperature of 31 °C.

$$\varepsilon = \frac{\dot{Q}_{gc,actual}}{\dot{Q}_{gc,max}} = \frac{h_{CO_2,gc,i} - h_{CO_2,gc,o}}{h_{CO_2,gc,i} - h_{CO_2}(P_{CO_2,gc}, T_{w,gc,i})} \quad (2)$$

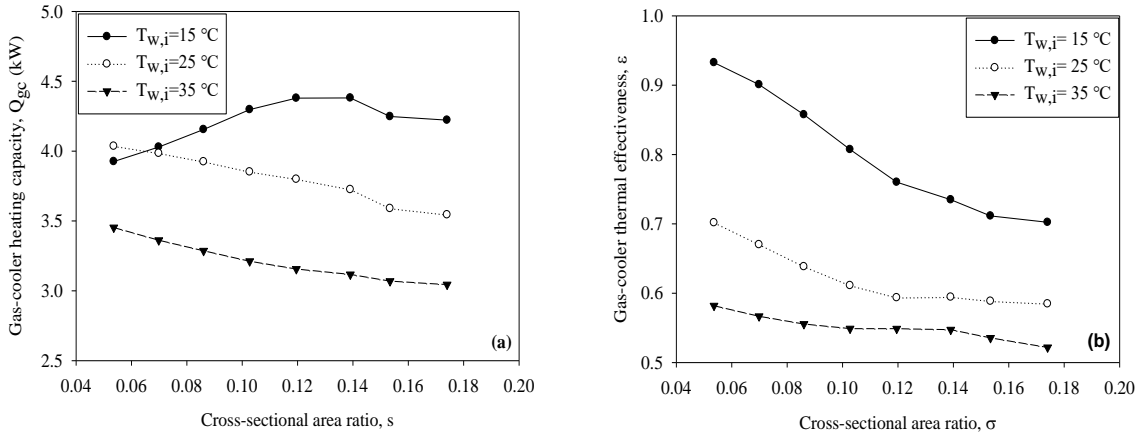


Fig. 6. Effects of the cross-sectional area ratio on (a) gas-cooler heating capacity and (b) gas-cooler thermal effectiveness (P_{gc}=9.5 MPa, rpm=3600, V_w=4 l/min).

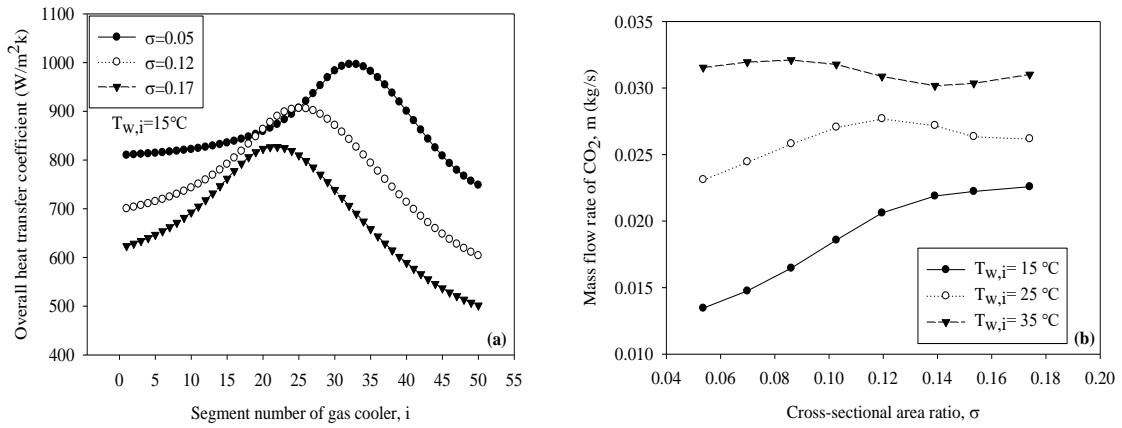


Fig. 7. Effects of the cross-sectional area ratio on (a) overall heat transfer coefficient in gas-cooler and (b) CO₂ mass flow rate (P_{gc}=9.5 MPa, rpm=3600, V_w=4 l/min).

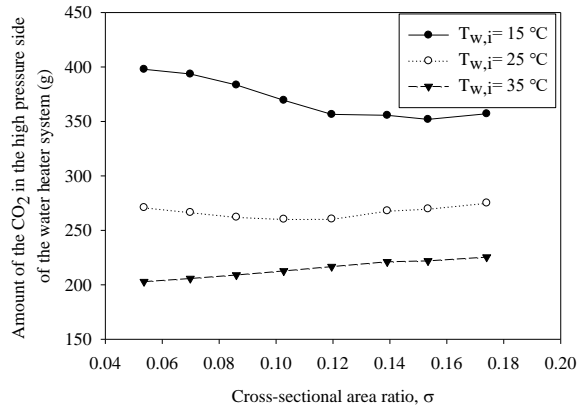


Fig. 8. Effect of the cross-sectional area ratio on CO₂ mass in the high pressure side of the water heater (P_{gc}=9.5 MPa, rpm=3600, V_w=4 l/min).

5. Conclusions

In this study, a numerical model of the CO₂ water heater system was developed and validated using the measured data for three different gas-coolers with three different GCARs. The isentropic efficiency and discharge temperature of the compressor were calculated by the neural network based on the experimental data. The numerical model of the water-CO₂ gas-cooler was developed by the finite volume method. The relative error of the heating capacity was lower than 10% and the water temperature at the gas-cooler outlet was lower than 3°C. The simulation results showed the increase in the gas-cooler thermal effectiveness with a decrease in the GCAR due to the increase in the heat transfer coefficient in the gas-cooler. When the CO₂ temperature at the gas-cooler outlet was lower than the pseudo-critical temperature (31 °C), the amount of the refrigerant in the high pressure side increased due to the increase in the CO₂ density between the gas-cooler and EEV. With the increase in the refrigerant in the high pressure side, the evaporating pressure decreased due to the lack of the refrigerant in the low pressure side. Therefore, the mass flow rate decreased with a decrease in the CO₂ density at the compressor inlet. Consequently, the heating capacity of the gas-cooler decreased. Overall, in order to optimize the gas-cooler having the maximum heating capacity, the GCAR should be maintained at 0.05 for the larger thermal effectiveness of the gas-cooler and higher CO₂ temperature at the gas-cooler outlet than the pseudo-critical temperature of CO₂ (31°C).

Acknowledgements

This work was supported by the Human Resources Program in Energy Technology of the Korea Institute of Energy Technology Evaluation and Planning (KETEP) grant financial resource from the Ministry of Trade, Industry & Energy, Republic of Korea. (No. 20144010200770).

Nomenclature

A	area (m ²)	Subscripts	
D	diameter (mm)	<i>as</i>	assumed
h	enthalpy (kJ/kg)	<i>comp</i>	compressor
i	segment number	<i>CO2</i>	carbon-dioxide
L	length (m)	<i>cr</i>	cross-sectional
\dot{m}	mass flow rate (kg/s)	<i>ev</i>	evaporation
n	tube number (-)	<i>gc</i>	gas-cooler
p	pressure (kPa)	<i>i</i>	inner, inlet

Q	heating capacity (kW)	<i>isen</i>	isentropic
rpm	compressor speed (rpm)	<i>max</i>	maximum
<i>T</i>	temperature (°C)	<i>o</i>	outer, outlet
Th	thickness (mm)	<i>r</i>	ratio
\dot{V}	volumetric flow rate (m ³ /s)	<i>sim</i>	simulated
		<i>sf</i>	surface
Greek symbols		<i>sh</i>	superheat
ε	thermal effectiveness (-)	<i>vol</i>	volumetric
σ	gas-cooler cross-sectional area ratio (-)	<i>w</i>	water
η	efficiency (-)		

References

- [1] Kauf F. Determination of the optimum high pressure for transcritical CO₂-refrigeration cycles. *Int J. Therm Sci* 1999;38:325-30.
- [2] Cecchinato L, Corradi M, Minetto S. A critical approach to the determination of optimal heat rejection pressure in transcritical systems. *Applied Thermal Engineering* 2010;30:1812-23.
- [3] D Sanchez, R Cabello, R Llopis, E Torrella. Development and validation of a finite element model for whater-CO₂ coaxial gas-coolers. *Applied Energy* 2012;93:637-47.
- [4] Gnielinski, Volker. New equations for heat and mass-transfer in turbulent pipe and channel flow. *International chemical engineering* 1976;16.2:359-68.
- [5] Stephan, Kr. Wärmeübergang bei turbulenter und bei laminarer Strömung in Ringspalten. *Chemie Ingenieur Technik* 1962;34.3:207-12.
- [6] Gnielinski, Akad Dir Dr-Ing Volker. Ein neues Berechnungsverfahren für die Wärmeübertragung im Übergangsbereich zwischen laminarer und turbulenter Rohrströmung. *Forschung im Ingenieurwesen* 1995;61.9:240-8.